Soft Matter

Accepted Manuscript

ROYAL SOCIETY OF CHEMISTRY

www.rsc.org/softmatter

Graphical Abstract

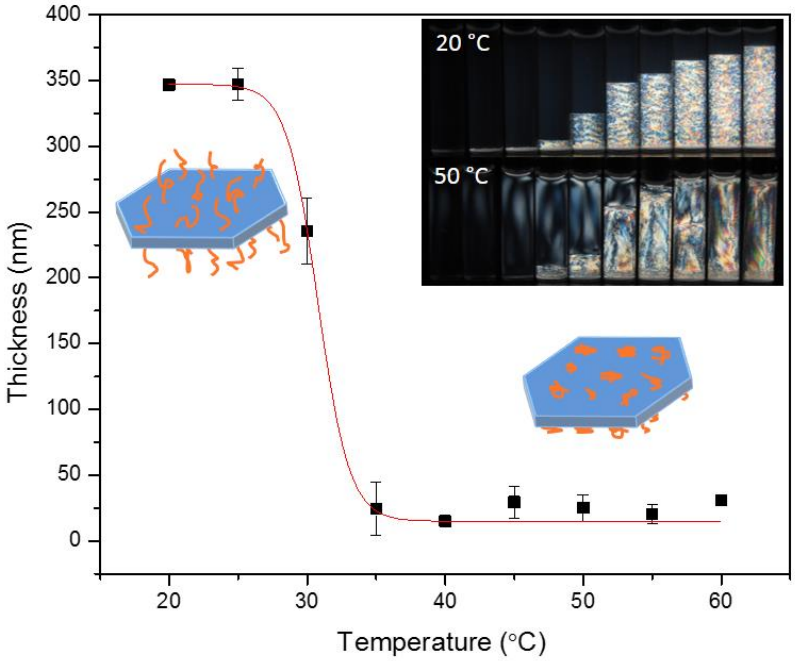

Temperature adjusts the thickness of ZrP-PNIPAM platelets, and reveals that soft disks self-assemble into nematic liquid crystals in a wider thickness-over-diameter ratio than do hard disks.

Soft Matter

RSCPublishing

COMMUNICATION

Thermo-sensitive Discotic Colloidal Liquid Crystals

Cite this: DOI: 10.1039/x0xx00000x

Xuezhen Wang[a], Di Zhao[b], Agustin Diaz[c], Ilse B. Nava Medina[d], Huiliang Wang[b], Zhengdong Cheng[adef]

Received 00th April 2014,
Accepted 00th January 2014

DOI: 10.1039/x0xx00000x

www.rsc.org/

We fabricated for the first time thermo-sensitive discotic liquid crystals by grafting poly(*N*-isopropylacrylamide) (PNIPAM) onto the zirconium phosphate (ZrP) platelets using pre-irradiated polymerization. The I-N transition was investigated by adjusting temperature for a single set of samples. We found that soft disks self-assemble into nematic liquid crystals in a wider thickness-over-diameter ratio than do hard disks.

Since Langmuir discovered in 1938 that clay particles exhibit a discotic nematic phase,[1] discotic liquid crystals of colloidal suspensions have been a growing field of scientific investigation.[2] Onsager predicted platelets could make an isotropic-to-nematic (I-N) transition.[3] Computer simulations of the I-N transition have been performed for discotic particles with different aspect ratios.[4] Lekkerkerker *et al.* obtained different liquid crystal phases, including nematic and columnar phases, from toluene suspensions of discotic gibbsite particles.[5] Graphene oxide aqueous suspensions have also been investigated for the formation of liquid crystals.[6] Temperature-sensitive colloidal crystals of spheres show a long history of study. Monodispersed PNIPAM spheres have been used to investigate crystallization and melting by changing temperature.[7, 8] Temperature-sensitive discotic liquid crystals, however, had not been realized before. Our group studied charged ZrP platelets of various sizes to investigate the I-N phase transition.[9] Here, we grafted PNIPAM onto the ZrP platelets to obtain thermo-sensitive discotic liquid crystals. By adjusting the temperature, we were able to vary the aspect ratio of the ZrP-PNIPAM so that we could study the aspect ratio dependence of the I-N transition. Our results showed that the phase diagram of ZrP-PNIPAM was consistent with that predicted by the Onsager-Parsons theory, and the nematic phase shows up at a higher aspect ratio in soft disks than in hard disks.

Pristine layered alpha zirconium phosphate (α-ZrP) prepared via hydrothermal method was hexagonal in shape, and the size was around 1μm (SEM image of α-ZrP was shown in supplemental information, Fig. S1). Monolayer ZrP platelets were obtained by exfoliating α-ZrP with tetrabutylammonium hydroxide (TBAOH) in deionized (DI) water.[9] Pre-irradiation method was used to prepare the ZrP-PINPAM platelets.[10] Aqueous ZrP platelet suspensions were first irradiated with ^{60}Co γ-rays under O_2 ambience to produce peroxide groups on the ZrP surfaces(See Fig. S2 for UV-Vis spectra for peroxide groups[11]). The peroxide groups were later decomposed into free radicals by heating, enabling the initiation of polymerization of *N*-isopropylacrylamide monomers to form PNIPAM polymers (See Fig. S3 for the FTIR spectra of ZrP-PNIPAM).

The sizes of the ZrP-PNIPAM platelets were measured by dynamic light scattering (DLS). According to our previous study, the TBA-exfoliated ZrP platelets have a fixed thickness of 2.68 nm.[12] Grafting of PNIPAM polymer onto the ZrP surface changes the thickness of the ZrP-PNIPAM platelets. We assumed the lateral dimension of the ZrP was not affected by the PNIPAM grafting. The thickness of the ZrP-PNIPAM platelets at various temperatures, therefore, can be calculated by measuring the diffusion of the platelets using DLS. The diameter of the ZrP platelets used for PNIPAM grafting was 891±270 nm. Fig.1 shows how the thickness of the ZrP-PNIPAM platelets varied with increasing temperature from 20°C to 60°C. The thickness decreased suddenly around 35°C, and then varied slightly from 35°C to 60°C. It is well known that PNIPAM has a phase transition around 30°C. In our case, ZrP-PNIPAM reached its smallest thickness above 35°C.

The sketches in Fig.1 illustrate how the ZrP-PNIPAM behaves before and after phase transition temperature; in this case, at 20°C and 50°C, respectively. The PNIPAMs on the surface of ZrP platelets were one-end-anchored free polymer chains at 20°C, and shrank to become smaller polymer coils at 50°C. As a result, the thickness of the ZrP-PNIPAM decreased at higher temperature. We simply fitted the thickness data with a smooth curve, and obtained the thickness of ZrP-PNIPAM at 50°C, which was 14.8±2.4 nm. The thickness at 50°C was about 23.4 times thinner than that at 20°C.

A set of ZrP-PNIPAM aqueous suspensions with different concentrations was used to establish the phase diagram at 20°C, and then at 50°C. As the concentration increased, there was an I-N phase transition. The nematic phase would settle to the

bottom, while the isotropic phase would move to the top under gravity, since it is less dense than the nematic phase. It took about two days for the samples in the coexistence to show a clear I-N interface at 20°C, and about five days at 50°C. Fig. 2a presents the cross-polarizing graphs of the ZrP-PNIPAM at 20°C and 50°C, respectively. Both sets of samples were kept at target temperature for 5 days.

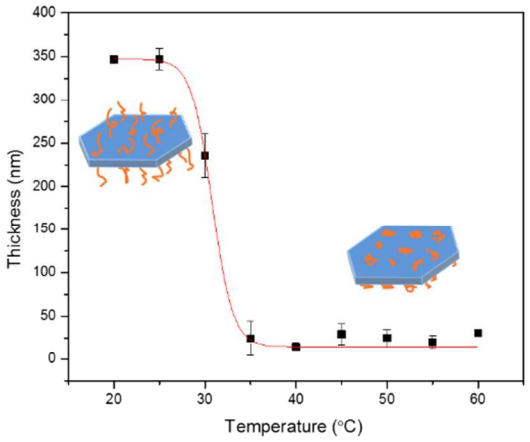

Fig. 1 The dependence of ZrP-PNIPAM platelet thickness on temperature. The temperature-dependent behavior of ZrP-PNIPAM is shown schematically.

The colorful nematic phase textures at 50°C were different from that at 20°C, as shown in Fig.2a. For the samples with concentrations of 0.00675, 0.0075, and 0.00825 (g/mL, particle to water), ZrP-PNIPAM showed sharp interfaces after 5 days at both temperatures. There were always sharp I-N interfaces for the ZrP-PNIPAM samples with higher concentrations, namely 0.009, 0.00975, 0.0105 and 0.012 g/mL at 20°C; however, at 50°C, higher concentration samples did not show interfaces, as they had a full nematic phase. The full nematic phase started to show up at a concentration of 0.00975 g/mL at 50°C. Nevertheless, even the highest concentration of ZrP-PNIPAM studied here did not have a full nematic phase at 20°C. The birefringent texture appearing in the isotropic phase at 50°C resulted from convection, which was induced by a temperature gradient since the photographs were taken at room temperature.

A diagram of nematic fraction of ZrP-PNIPAM platelets versus the volume fraction at 20°C (circle) and 50°C (square) were plotted in Fig. 2b. The conversion of concentrations of the ZrP-PNIPAM to their volume fractions can be found in the supplementary information. The nematic fractions were obtained using the equilibrium height of the nematic phase normalized by the sample heights. Since the nematic phase would be compressed with time due to gravity,[13] a time sequence of cross-polarizing photographs were taken for each single sample, then the equilibrium nematic fractions were obtained by extrapolating the time-dependent nematic fraction to time zero (the method of extrapolating can be found in Fig. S4).

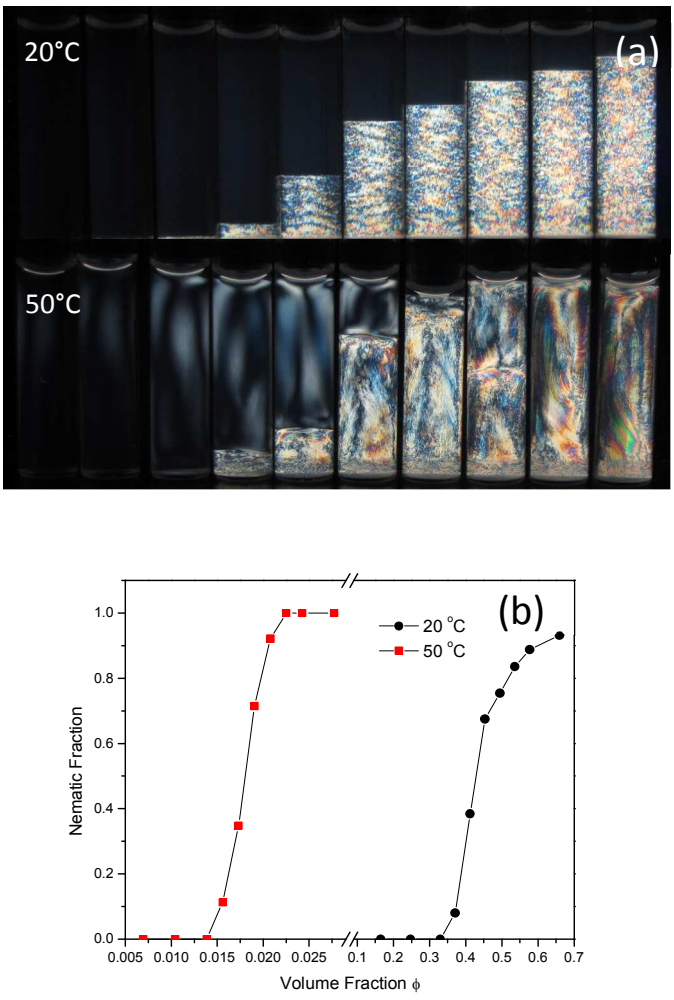

Fig. 2 (a) Cross-polarizing photographs of aqueous ZrP-PNIPAM suspensions at 20°C and 50°C. The ZrP-PNIPAM concentration from left to right: 0.003, 0.0045, 0.006, 0.00675, 0.0075, 0.00825, 0.009, 0.00975, 0.0105 and 0.012 g/mL. (b) The fraction of nematic phase as a function of the platelets volume fraction ϕ.

The phase diagram of ZrP-PNIPAM at 50°C shifted to lower volume fraction compared with 20°C. Also, the width of the I-N transition at 50°C was narrower than that at 20°C. According to previous research about the effect of the polydispersity of hard particles on the I-N transition, the larger particles preferred to stay in the nematic phase rather than in the isotropic phase, and the disparity in the number of larger to smaller particles in isotropic and nematic phase would increase as the polydispersity increased.[14] However, the polydispersity was the same for ZrP-PNIPAM at both 20°C and 50°C, which according to DLS result was 24±2%, since the same sample had been used for the investigation (see Fig. S5 for the size distribution).

In our case, the shrinking of PNIPAM on the ZrP surface at 50°C reduced the thickness of the ZrP-PNIPAM, hence their volume fraction. The reduction in thickness would decrease the aspect ratio (ξ), defined as the ratio of diameter over thickness, of the ZrP-PNIPAM since the diameter of the platelet did not change. The aspect ratio of ZrP-PNIPAM decreased from 0.386

to 0.0162 as the temperature increased from 20°C to 50°C. For the same polydispersity, the I-N transition width of ZrP-PNIPAM at 50°C with ξ=0.0162 was narrower than that of ZrP with ξ=0.01(Fig. S6a). However, for ZrP-PNIPAM with the same polydispersity, the width of the I-N transition was larger at higher aspect ratio, corresponding to 20°C, than that at 50°C (the qualitative difference can be found in Fig. S6a and S6b). This observation confirmed our previous result on charged ZrP platelets, the higher the aspect ratio, the wider the I-N transition width (Fig.S6c). [9]

To gain a better understanding on how the aspect ratio affects the ZrP-PNIPAM phase diagram, the I-N transition was also studied at 30°C. As shown in Fig. 1, the thickness of the ZrP-PNIPAM platelets were 346±3 nm, 235±25 nm, and 14.8±5.9 nm at 20°C, 30°C, and 50°C, respectively. The aspect ratio for the sample at 20°C was 1.5 times and 23.4 times larger than that at 30°C and 50°C, respectively. Obviously, the aspect ratio can be easily adjusted by temperature. The advantage of the ZrP-PNIPAM platelets is that we were able to use just one set of samples to study the phase diagram of the I-N transition with various aspect ratios.

Fig. 3 presents the log-log plot of the I-N transition volume fraction ϕ versus aspect ratio ξ of ZrP-PNIPAM platelets (red circles and solid fitting line). The ϕ-ξ curve for charged ZrP platelets[9] (black squares and solid fitting line), two curves of oblate hard spherocylinders (OHSC) free energy calculation[15] (green dotted lines), and Onsager-Parsons theory[16] curve (blue short dotted line) were also plotted for comparison. The ϕ-ξ of ZrP-PNIPAM can be fitted into a linear line, which had a similar tendency as the ϕ-ξ line of ZrP system,[9] OHSC free energy calculation, Onsager-Parsons theory, and the I-N transition of cut spheres.[4]

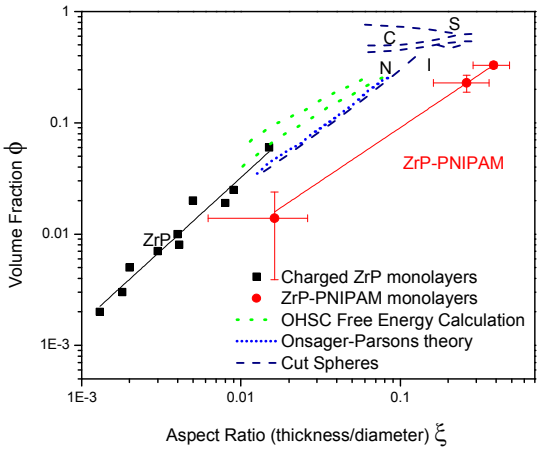

Fig. 3 The dependence of the I-N transition on aspect ratio.

The slopes of the OHSC free energy calculation curves are 3.81±0.11 and 3.12±0.78, respectively, while Onsager-Parsons theory has a similar slope of 3.15±0.05. The slope of charged ZrP platelets, 3.95±0.36, is close to the theoretical calculations, but the data is for a smaller aspect ratio range. The curves of charged ZrP and the Onsager-Parsons theory are consistent with each other, and might be two different parts of the same continuous curve. The slope of I-N transition curve for cut spheres[4] is 3.27±0.06, which is similar to the charged ZrP samples. The slope for ZrP-PNIPAM, 0.96±0.02, however, is significantly smaller than any of mentioned slopes. In addition, the phase diagram of cut spheres[4] indicates that liquid crystals exist only when ξ is smaller than 0.25, as shown in Fig. 3 (solid navy lines). For ξ =0.1, there were isotropic (I), nematic (N), columnar (C), and solid (S) phases; for ξ =0.2, there were isotropic, columnar, and solid phases; for ξ=0.3, there were only isotropic and solid phases. As observed here for the ZrP-PNIPAM soft platelets, the nematic phase still exists for aspect ratios as high as 0.33. Hence, by modifying with PNIPAM, charged ZrP platelets became soft ZrP-PNIPAM platelets, and the I-N transition curve shifts towards higher aspect ratio with a much less steep slope.

Conclusions

In summary, thermo-sensitive discotic liquid crystals were fabricated using the pre-irradiated polymerization of temperature-sensitive poly(*N*-isopropylacrylamide) (PNIPAM) on the surface of ZrP platelets. To the best of our knowledge, this is the first time that temperature-sensitive *discotic* liquid crystals were obtained. By changing environmental temperature, the thickness of the ZrP-PNIPAM was changed; the aspect ratio of ZrP-PNIPAM was about 23.4 times smaller at 50°C than at 20°C. As a result, the phase diagram of ZrP-PNIPAM platelets was shifted to lower volume fraction as temperature increased. The dependence of the I-N transition on the aspect ratio agrees with our previously result on charged ZrP platelets, as well as the OHSC free energy calculation and Onsager-Parsons theory. Moreover, we were able to study the I-N phase diagram in volume fraction versus aspect ratio by adjusting the temperature, using only one set of ZrP-PNIPAM samples. The nematic phase can exist at a higher aspect ratio for the soft ZrP-PNIPAM disks than for the hard cut spheres.

Experimental method

Hexagonal α-ZrP crystals with multiples layers were synthesized by the hydrothermal method.[17] ZrP platelets (around 1 μm in diameter) were obtained by exfoliating 1g of α-ZrP crystals in 30 mL water using 2.2 mL 40%wt tetrabutylammonium hydroxide (TBAOH). The molar ratio of ZrP to TBAOH is 1:1. The aqueous ZrP platelets suspensions with a concentration of 0.03 g/mL were then irradiated with ^{60}Co γ-rays (dose rate: 5 kGy/h) under oxygen flow for 6 h to generate peroxide groups on the surface of the ZrP platelets.

An aqueous suspension of 5 mL containing 2.5 mL of ^{60}Co γ-rays irradiated ZrP platelets and 0.1 g *N*-isopropylacrylamide (re-crystallized in a mixture of toluene and hexane) were added to a 10-mL test tube with a septum stopper. The mixture was purged with nitrogen bubbling for 20 min. The sealed test tube was then placed in a 50°C water bath, where the polymerization

reaction continued for 24 h. The produced ZrP-PNIPAM platelets were centrifuged, washed with deionized water twice, and resuspended in water for further analysis. The sizes of the ZrP-PNIPAM platelets at different temperatures were measured using dynamic light scattering (DLS, Malvern Instruments Ltd, UK).

ZrP-PNIPAM suspensions of 1 mL with different particle concentrations were prepared by diluting a mother sample with deionized water. The samples were then put into an oven (Napco vacuum oven, Model 5831) with the target temperatures (20°C, 35°C, and 50°C) under atmospheric conditions. Sample photographs were taken with sample set briefly outside the oven between a cross-polarizer and a fluorescent light shining from behind.a

Acknowledgements

This work is partially supported by NSF (DMR-1006870) and NASA (NASA-NNX13AQ60G). X.Z. Wang acknowledges support from the Mary Kay O'Connor Process Safety Center (MKOPSC) at Texas A&M University.

Notes and references

[a]Artie McFerrin Department of Chemical Engineering, Texas A&M University, College Station, TX, 77843-3122, USA. E-mail: zcheng@tamu.edu
[b]College of Chemistry, Beijing Normal University, Beijing, 100875, China
[c]Department of Chemistry, Texas A&M University, College Station, TX 77843-3125, USA.
[d]Materials Science and Engineering, Texas A&M University, College Station, TX, 77843-3003, USA
[e]Mary Kay O'Connor Process Safety Center, Artie McFerrin Department of Chemical Engineering, Texas A&M University, College Station, TX, 77843-3122, USA
[f]Soft Matter Center, Guangdong Provincial Key Laboratory on Functional Soft Matter, School of Materials and Energy, Guangdong University of Technology, Guangzhou, 510006, China

Electronic Supplementary Information (ESI) available: [UV-Vis spectra for peroxide groups and FTIR spectra for ZrP-PNIPAM sample, sedimentation procedure to obtain the equilibrium nematic fraction for the ZrP-PNIPAM samples, DLS size distribution, I-N transition of ZrP-PNIPAM and ZrP versus polydispersity, Isotropic volume fraction ϕ_I-ξ and nematic volume fraction ϕ_N-ξ of ZrP-PNIPAM and ZrP]. See DOI: 10.1039/b000000x/

References

1 Langmuir, *J. Chem. Phys.*, 1938, **6**, 873-896.
2 H. N. W. Lekkerkerker and G. J. Vroege, *Phil. Trans. R .Soc. A*, 2013, **371**, 20120263-20120263.
3 L. Onsager, *Ann. N.Y. Acad. Sci.*, 1949, **51**, 627-659.
4 J. A. C. Veerman and D. Frenkel, *Phys. Rev. A*, 1992, **45**, 5632-5648.
5 F. M. van der Kooij, K. Kassapidou and H. N. W. Lekkerkerker, *Nature*, 2000, **406**, 868-871.
6 J. E. Kim, T. H. Han, S. H. Lee, J. Y. Kim, C. W. Ahn, J. M. Yun and S. O. Kim, *Angew. Chem., Int. Ed.*, 2011, **50**, 3043-3047.
7 A. M. Alsayed, M. F. Islam, J. Zhang, P. J. Collings and A. G. Yodh, *Science*, 2005, **309**, 1207-1210.
8 S. Tang, Z. Hu, Z. Cheng and J. Wu, 2004, *Langmuir*, **20**, 8858-8864.
9 A. F. Mejia, Y. W. Chang, R. Ng, M. Shuai, M. S. Mannan and Z. D. Cheng, *Phys. Rev. E*, 2012, **85**, 061708.
10 T. Huang, H. Xu, K. Jiao, L. Zhu, H. R. Brown and H. Wang, *Adv. Mater.*, 2007, **19**, 1622-1626.
11 H. Lee, J. Ryu, D. Kim, Y. Joo, S. U. Lee and D. Sohn, *J. Colloid Interface Sci.*, 2013, **406**, 165-171.
12 P. He, A. F. Mejia, Z. Cheng, D. Sun, H.-J. Sue, D. S. Dinair and M. Marquez, *Phys. Rev. E*, 2010, **81**, 026310.
13 H. H. Wensink and H. N. W. Lekkerkerker, *Europhys. Lett.*, 2004, **66**, 125-131.
14 M. A. Bates and D. Frenkel, *J. Chem. Phys.*, 1999, **110**, 6553-6559.
15 M. Marechal, A. Cuetos, B. Martínez-Haya and M. Dijkstra, *J. Chem. Phys.*, 2011, **134**, 094501.
16 H. H. Wensink and H. N. W. Lekkerkerker, *Mol. Phys.*, 2009, **107**, 2111-2118.
17 M. Shuai, A. F. Mejia, Y.-W. Chang and Z. Cheng, *CrystEngComm*, 2013, **15**, 1970-1977.

